Heliyon 11 (2025) e42537

Contents lists available at ScienceDirect

Heliyon

journal homepage: www.cell.com/heliyon

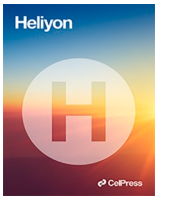

Case report

Rapid development of acute monocytic leukemia (AML-M5b) with t(9;11)(p22;q23) after chemotherapy for T-cell lymphoblastic lymphoma: A case report

Jiao Cai [a,1], Nan Zhang [a,1], Ling Qiu [a,1], Bai-tao Dou [a,b], Meng-jiao Li [a,b], Dan Chen [a], Shi-hui Ren [a], Lei Ma [a], Hao Yao [a,b,**], Fang-yi Fan [a,b,*]

[a] *Department of Hematology, Chinese People's Liberation Army The General Hospital of Western Theater Command, Chengdu, SiChuan, 610083, China*

[b] *Department of Clinical Medicine, North Sichuan Medical College, Nanchong, SiChuan, China*

A R T I C L E I N F O

Keywords:
Case report
T-cell lymphoblastic lymphoma
AML
Whole-exome sequencing
t(9
11)(p22
q23) translocation
SETD2

A B S T R A C T

Objective: To investigate the diagnosis and treatment of T lymphoblastic lymphoma (T-LBL) progressing into acute monocytic leukemia (AML-M5b) and explore possible pathogenic mechanisms.

Methods: Comprehensive diagnosis and evaluation of the patient's disease status were conducted through lymph node biopsy, bone marrow aspiration and biopsy, PET/CT, immunohistochemistry, flow cytometry, fusion gene detection, and whole-exome sequencing (WES) based on the clinical manifestations at different stages.

Results: The lymph node biopsy revealed Ki67 positivity at 80 % and expression of TDT, CD4, CD8, CD3, and CD5. The PET/CT scan showed increased FDG metabolism at multiple sites. Based on relevant tests and examination results, the patient was diagnosed with T-LBL (stage IV; IPI score, 3). After three cycles of chemotherapy, abnormal immature monocytes were detected using bone marrow flow cytometry, suggesting an acute progression from T-LBL to AML-M5b. Chromosomal karyotype analysis revealed t(9; 11)(p22; q23) and the MLL-AF9 fusion gene. WES analysis identified mutations in several genes, among which mutations in SET domain-containing protein 2 and CBL may be associated with the occurrence of acute myeloid leukemia. The patient died 1 month after AML-M5b diagnosis.

Conclusion: Patients with T-LBL progression to AML have a poor prognosis and shorter overall survival. Hence, exploring the pathogenic mechanisms and reasons for disease progression has significant implications for finding effective treatment modalities and prolonging patient survival.

* Department of Hematology, General Hospital of the Chinese People's Liberation Army Western Theatre, No. 270, Rongdu Avenue, Chengdu, Sichuan Province, 610083, China.

** Department of Hematology, General Hospital of the Chinese People's Liberation Army Western Theatre, No. 270, Rongdu Avenue, Chengdu, Sichuan Province, 610083, China.

E-mail addresses: yaohao9001@163.com (H. Yao), 834525469@QQ.com (F.-y. Fan).

[1] These authors have contributed equally to this work and share first authorship.

https://doi.org/10.1016/j.heliyon.2025.e42537
Received 3 March 2024; Received in revised form 17 October 2024; Accepted 6 February 2025
Available online 9 February 2025

1. Introduction

T lymphoblastic lymphoma (T-LBL) is a highly invasive subtype of non-Hodgkin lymphoma (NHL) that commonly involves the mediastinum, bone marrow, and central nervous system. It progresses rapidly and has poor prognosis. Here, we report a case of T-LBL that was followed by the development of acute monocytic leukemia (AML-M5b), treated at our hospital. We aimed to explore the molecular mechanisms underlying the progression from T-LBL to AML, along with its clinical manifestations, diagnostic methods, and treatment strategies before and after this progression, to identify effective therapeutic approaches and improve patient survival.

2. Case report

A male patient in his late twenties presented to our hospital with complaints of swollen inguinal lymph nodes lasting for several months. Multiple enlarged lymph nodes were observed in both inguinal regions, without tenderness or fever. On May 16, the patient underwent blood tests at Ya'an People's Hospital, which revealed a white blood cell count of 51.7×10^9/L, a hemoglobin level of 119

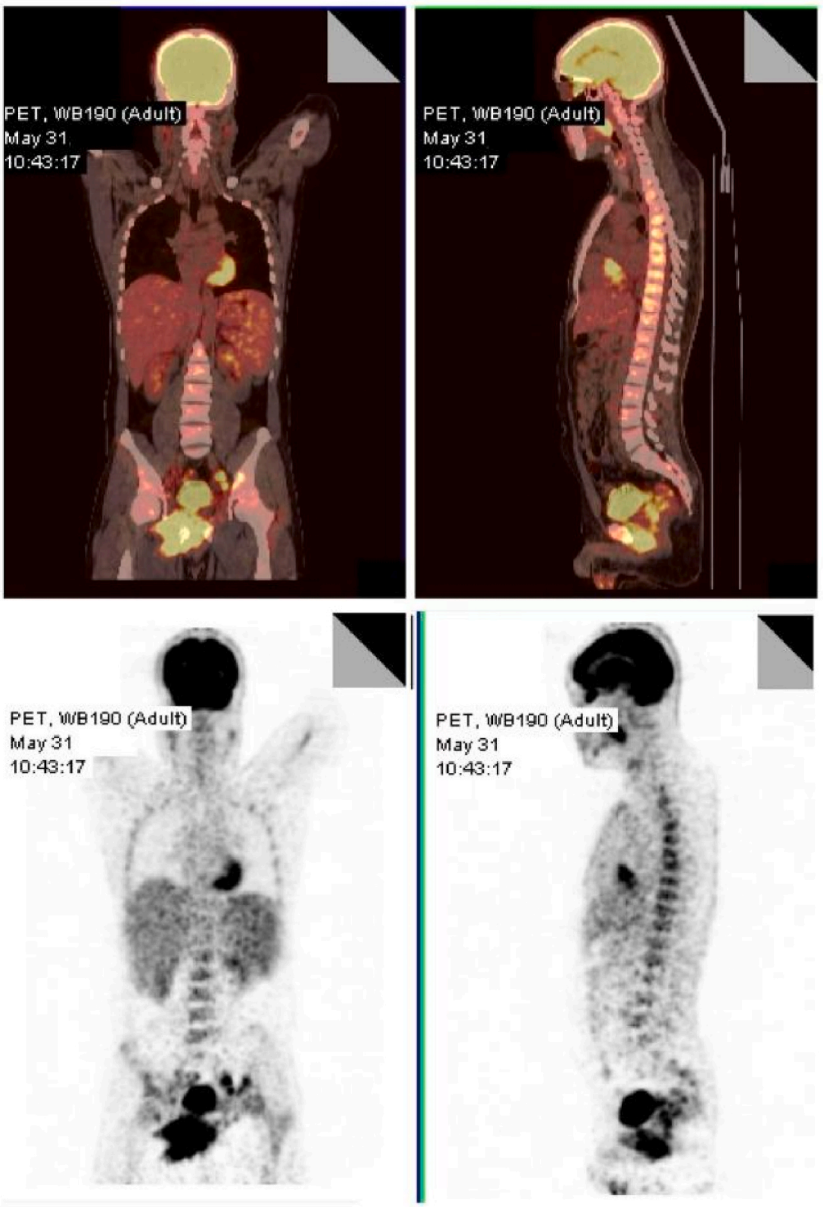

Fig. 1. PET/CT and 18F-FDG uptake imaging.

g/L, and a platelet count of 78 × 10^9/L. Chest and abdominal enhanced CT scans revealed multiple enlarged lymph nodes in both inguinal regions, predominantly on the right side, with the largest measuring approximately 2.8 cm in diameter. Additionally, multiple lymph nodes were observed in the pelvic cavity. Rectal wall thickening with indistinct fat planes and increased density suggestive of space-occupying lesions were noted. Destruction of the right pubic symphysis and swelling of the surrounding soft tissue were observed, with a suspected space-occupying lesion. A bone marrow smear revealed significantly active myeloid cell proliferation with a high granulocyte-to-red cell ratio, a predominance of intermediate to mature granulocytes, and abundant eosinophils without basophils. Flow cytometry analysis of the bone marrow showed an increased proportion of granulocytes (91.7 %, predominantly immature granulocytes), with suspected eosinophils accounting for 39.5 %. Fusion gene detection for BCR-ABL was negative. On May 20, a right inguinal lymph node biopsy was performed, and the pathological and immunohistochemical results indicated tumor cells positive for CD2 (partially +), CD8 (+), CD3 (diffuse +), CD4 (partially +), CD20 (−), CD30 (−), CD56 (−), CD10 (−), CD21 (occasional residual FDC meshwork), Granzyme-B (−), Bc1–6 (−), PD-1 (−), EMA (−), κ (+), λ (−), PAX-5 (−), MPO (scattered, focal +), CD68 (scattered +), and Ki-67 (+, approximately 90 %). The pathological diagnosis was peripheral T-cell lymphoma, which was not specified otherwise. The patient had no significant medical history, although his father passed from lung cancer. Physical examination revealed bilateral scattered soft inguinal lymph node enlargement with palpable and movable masses. Enlarged, soft, and mobile lymph nodes were palpable in the left cervical region.

Upon admission, the patient's laboratory findings revealed a white blood cell count of 56.30 × 10^9/L, red blood cell count of 3.70 × 10^{12}/L, hemoglobin concentration of 111 g/L, and platelet count of 133 × 10^9/L. Other laboratory parameters included procalcitonin 0.19 ng/ml; lactate dehydrogenase 400.1 IU/L; liver function tests showed total bilirubin 4.4 μmol/L, direct bilirubin 2.6 μmol/L, indirect bilirubin 1.9 μmol/L, alanine aminotransferase 109.6 IU/L, and aspartate aminotransferase 52.8 IU/L; renal function tests showed urea 8.71 mmol/L and uric acid 515 μmol/L. Cytokine analysis revealed an interleukin-8 level of 1504.00 pg/mL. Serological tests for infectious diseases showed positivity for the hepatitis C core antigen. β2 microglobulin, coagulation parameters, and thromboelastography were within normal limits.

PET-CT scan performed on May 31, revealed the following: 1. Osteolytic bone destruction with surrounding soft tissue swelling and increased FDG metabolism around the right pubic and ischial bones, measuring approximately 10.2 cm × 8.8 cm × 7.4 cm, with markedly increased radiotracer uptake, maximum SUV approximately 12.5, and average SUV approximately 6.7; multiple enlarged lymph nodes were detected in the bilateral neck, pelvic walls, bilateral iliac fossae, and bilateral inguinal regions, with the largest measuring approximately 3.1 cm × 2.4 cm, maximum SUV approximately 5.1, and average SUV approximately 2.5. These lesions showed varying degrees of increased radiotracer uptake, suggesting lymphoma. 2. A diffuse increase in FDG metabolism within the bone marrow cavities of the bilateral humeral shafts, bilateral clavicles, spine, pelvic bones, and bilateral proximal femurs was observed without definitive bone destruction. The spleen showed increased volume with a diffuse elevation in FDG metabolism. These findings were consistent with lymphoma (Fig. 1).

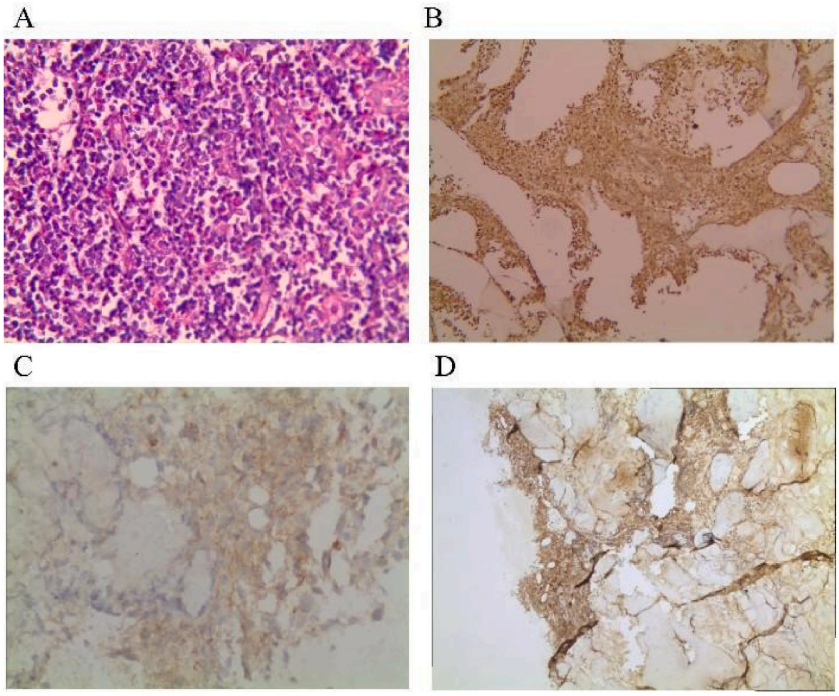

Fig. 2. Histopathological features of T-LBL.
A: Diffuse proliferation of tumor cells is observed microscopically. The tumor cells demonstrate marked pleomorphism with eosinophilic cytoplasm and deeply stained nuclei. Locally, the tumor cells exhibit a cord-like distribution.

A bone marrow smear on June 4, showed markedly active myeloid cell proliferation and an increased proportion of eosinophils, with 3 % of the eosinophils exhibiting blue-black cytoplasmic basophilic granules. A bone marrow biopsy revealed active bone marrow cell proliferation and significant myeloid cell proliferation. Immunohistochemical staining showed the expression of Glycophorin A and E-Cadherin in erythroid cells; MPO in myeloid cells; CD61 in megakaryocytes; variable expression of CD20, CD3, and TdT in lymphocytes; CD138 in plasma cells; and focal expression of CD34 and CD117.

On June 3, the patient received the CHOEP regimen chemotherapy (cyclophosphamide 1.45 g on day 1; doxorubicin 95 mg on day 1; vincristine 4 mg on day 1, etoposide 0.1 g on days 1–3, prednisone 75 mg on days 1–5). On June 12, pathological consultation at our hospital revealed an NHL involving the right inguinal lymph node. Immunohistochemical staining showed tumor cells positive for Ki67 (80 %), TDT, CD4, CD8, CD3, CD5, and CD45 and negative for CD21, CD15, bcl-2, PAX-5, CD30, Bc1–6, CD10, PD-1, CXCL-13, and EBER. The pathological diagnosis was a T-LBL involving the right inguinal lymph node (Fig. 2). The clinical diagnosis was T-LBL (stage IV; IPI score, 3).

On July 16, the patient underwent chemotherapy with the BFM regimen, which consisted of prednisone 120 mg on days 1–28 (halved every 3 days from day 9 onwards until completion); vincristine 4 mg on days 8, 15, 22, and 29; doxorubicin 60 mg on days 8, 15, 22, and 29; pegaspargase 3750 IU on day 12; cyclophosphamide 2000 mg on days 36 and 64; cytarabine 150 mg on days 38–41, 45–48, 52–55, and 59–62; mercaptopurine 120 mg on days 36–63; and intrathecal triple therapy on days 1, 15, 29, 45, and 59.

On October 17, the patient received chemotherapy with the BFM-90 regimen, including oral mercaptopurine 50 mg daily from days 1–56; intravenous methotrexate 10 g on days 8, 22, 36, and 50; and intrathecal methotrexate 10 mg on days 8, 22, 36, and 50.

On November 8, the patient was admitted with a white blood cell count of 118.31×10^9/L, red blood cell count of 3.79×10^{12}/L, hemoglobin concentration of 121 g/L, and platelet count of 40×10^9/L. Subsequent ultrasound examination of the superficial lymph nodes revealed enlargement of the lymph nodes in the left cervical regions (levels I-IV) and right cervical regions (levels III-V), as well as in the bilateral inguinal regions. Bone marrow smear showed significantly active myeloid cell proliferation, with lymphoma cells comprising 74 % of the total cell population. Flow cytometry analysis of the bone marrow revealed approximately 81.6 % abnormal cells expressing HLA-DR, CD64, CD11c, CD4, CD33, and CD38, with partial expression of CD9, dim CD123, dim CD15, CD13, CD56, and CD11b and minimal expression of CD14. These cells were identified as a mixture of abnormal immature and mature monocytes, predominantly immature, with aberrant CD56 expression. The presence of abnormal immature monocytes with the detected MLL-AF9 fusion gene suggests a case of acute monocytic leukemia (AML-M5b), which may have developed following chemotherapy for T-LBL. A subsequent bone marrow smear on November 19, showed immature monocytes comprising 67.5 % of the cell population. Screening for leukemia-associated fusion genes revealed positivity for MLL-AF9.

Flow cytometry analysis conducted on November 19, indicated 57.67 % malignant immature monocytes expressing MPOdim, CD33, CD11b, HLA-DR, CD64, CD11c, CD15, CD38, CD371, CD123, CD4, and CD36; partial expression of CD13 and CD56; and the absence of CD22, cCD3, CD34, CD7, CD117, CD3, CD14, CD96, CD110, CD5, CD2, CD61, CD42a, CD9, cCDT, and CD24. Granulocytes comprised 20.03 % of the cell population; mature monocytes, 2.97 %; eosinophils, 1.20 %; and nucleated red blood cells, 9.37 %. Consequently, the patient was diagnosed with AML-M5b.

Leukemia mutation screening revealed mutations in CBL (mutation frequency, 50.5 %) and SET domain-containing protein 2 (SETD2) (mutation frequency, 51.4 %). Chromosomal analysis showed a karyotype of 46, XY, t(9; 11)(p22; q23).

On November 26, the patient received chemotherapy with an IDA regimen (idarubicin 20 mg on days 1–3, cytarabine 300 mg on days 1–7). However, the tumor continued to progress, and the patient succumbed to AML-M5b 1 month after diagnosis.

3. Discussion

T-LBL is a rare subtype of NHL with low incidence rates. It primarily affects children and adolescents, with a higher prevalence in men, and is extremely rare in adults. The pathogenesis of T-LBL may be attributed to various biological processes, including genetic mutations and epigenetic abnormalities, which lead to sustained proliferation, self-renewal, and blockade of the differentiation of immature precursor T cells [1].

In this case, the patient's progression from T-LBL to AML-M5b was accompanied by the detection of the MLL-AF9 fusion gene resulting from a t(9; 11)(p22; q23) chromosomal translocation. In acute leukemia, MLL can form fusion proteins with over 50 genes through chromosomal translocation, thus participating in the development of different subtypes [2]. The MLL fusion gene acts as an oncogene by enhancing cell proliferation and inhibiting the differentiation of hematopoietic stem cells, leading to a poor prognosis in acute leukemia patients [3]. The oncogenic potential of MLL fusion genes is regulated by various factors including signaling proteins [4,5], epigenetic regulators [6], and transcription factors [7]. Besides, The aberrant expression of kappa light chains in a T-cell malignancy, as observed in this case, has been documented in rare instances. Such expression may reflect a dysregulated immunophenotypic profile in aggressive lymphomas, warranting further investigation into its biological significance. Despite this unusual finding, the strong expression of T-cell markers (CD3, CD4, CD8) confirms the diagnosis of T-LBL.

After conducting whole-exome sequencing analysis, mutations in multiple genes were identified in lymph node biopsy samples of the patient diagnosed with T-LBL, including NOTCH1, BRCA1, CBL, DDR2, MYO5A, and SETD2 (Table 1). Bioinformatic comparison analysis with various databases, such as COSMIC, CIViC, PharmGKB, and dbSNP, revealed that mutations in SETD2 and CBL may be associated with the development of myeloid leukemia.

CBL is an oncogene located on chromosome 11q23.3. The protein product features an N-terminal domain that interacts with tyrosine kinases, thereby facilitating the degradation of various substrates through the proteasomal pathway. Additionally, it contains a RING domain, which serves as an E3 ubiquitin ligase that is crucial for maintaining cellular homeostasis. CBL negatively regulates tyrosine kinase signaling via its ubiquitination activity, activates RAS and PSTAT5, and influences the stability and signaling of JAK2

Table 1
Gene mutations detected via whole exome sequencing.

Gene	Transcript ID	Chromosome	Exon Mutation	Nucleotide Mutation	Amino Acid Mutations	dbSNP
NOTCH1	NM_017617	9	34	c.6751G > A	p.A2251T	2.60 %
BRCA1	NM_007294	17	23	c.5521delA	p.S1841fs	48.90 %
CBL	NM_005188	11	9	c.1318G > A	p.G440S	47.60 %
DDR2	NM_006182	1	6	c.512A > G	p.D171G	53.30 %
FAT1	NM_005245	4	19	c.11245G > A	p.D3749N	2.20 %
GRM3	NM_000840	7	3	c.984G > C	p.Q328H	49.70 %
HIST1H2BC	NM_003526	Chr6	1	c.211_212insAACGACATAT	p.F71_E72delinsX	39.00 %
IKZF3	NM_012481	17	8	c.1087A > G	p.S363G	48.80 %
LRP1B	NM_018557	2	38	c.6030G > T	p.L2010F	49.40 %
MYO5A	NM_000259	15	20	c.2431T > A	p.F811I	52.00 %
PCLO	NM_033026	7	2	c.1123_1124insCTCTTGGTCCTGCTAAGCCTCCAGCTCAGC	p.Q375delinsPLGPAKPPAQQ	44.20 %
SETD2	NM_014159	3	3	c.2399G > A	p.S800N	47.50 %

[8,9].

Loss or inactivating mutations in the CBL gene have been observed in various myeloid malignancies, including myelodysplastic syndrome [10], myeloproliferative neoplasms [11], AML [12], atypical chronic myeloid leukemia, juvenile myelomonocytic leukemia [13], and chronic myelomonocytic leukemia (CMML) [14]. In CMML, CBL mutations occur relatively frequently, accounting for approximately 20 % of cases, and are strongly associated with progression to AML and poor prognosis [15].

SETD2 is the only known trimethyltransferase responsible for the formation of H3K36me3. The main functions of SETD2/H3K36me3 include DNA damage repair, maintenance of chromatin activity, and facilitation of transcriptional elongation to promote gene transcription. Sanger sequencing of 134 cases of AML and 107 cases of acute lymphoblastic leukemia revealed that 22.2 % of patients with MLL fusion protein-associated leukemia harbored SETD2 mutations. Furthermore, 86.7 % of the patients with SETD2 mutations harbored other chromosomal abnormalities known to promote the development of leukemia. Downregulation of SETD2 under conditions of genetic damage can enhance the self-renewal potential of leukemia stem cells, thereby promoting leukemia progression. Disruption of the SETD2-H3K36me3 signaling pathway represents a unique epigenetic mechanism in leukemia development.

Protein interaction analysis of seven MLL fusion proteins (MLL-AF1p, MLL-AF4, MLL-AF9, MLL-CBP, MLL-EEN, MLL-ENL, and MLL-GAS7) revealed significant involvement of SETD2 in the occurrence and development of MLL fusion protein-associated leukemia. Interestingly, through a series of in vivo and in vitro experiments, researchers discovered that the complete loss of SETD2 could induce apoptosis, differentiation, and proliferation inhibition of AML cells by inhibiting the activity of the H3K79 methyltransferase DOT1L, leading to increased DNA damage. Homozygous loss of SETD2 significantly prolonged the latency to leukemia onset, whereas heterozygous loss accelerated MLL-AF9-induced leukemia development and led to resistance to cytarabine chemotherapy.

In summary, mutations in multiple genes, such as CBL and SETD2, may promote the formation of MLL fusion proteins and the progression of T-LBL to AML-M5b via regulation of multiple signaling pathways, transcription factors, epigenetic regulators, and various levels of transcription, translation, and epigenetic modifications. In this case, the disease progressed rapidly; the patient was insensitive to chemotherapy and had a short overall survival (Table 2).

CRediT authorship contribution statement

Jiao Cai: Writing – original draft, Investigation, Formal analysis. **Nan Zhang:** Investigation, Formal analysis. **Ling Qiu:** Investigation, Formal analysis. **Bai-tao Dou:** Project administration, Methodology. **Meng-jiao Li:** Project administration, Methodology. **Dan Chen:** Project administration, Funding acquisition. **Shi-hui Ren:** Methodology. **Lei Ma:** Project administration. **Hao Yao:** Writing – review & editing, Validation, Funding acquisition. **Fang-yi Fan:** Writing – review & editing, Conceptualization.

4. Ethics approval and consent to participate

The study protocol was reviewed, and the need for approval was waived by the Ethics Committee of the People's Liberation Army, The General Hospital of Western Theater Command.

Table 2
Patient disease progression and treatment process.

Date	Lesion Site	Immunophenotype	Diagnosis	Karyotype	Treatment Regimen
May 20	Right inguinal lymph node	Ki67 (+, 90 %), CD8 (+), CD3 (diffuse+), CD2 (partial+), CD4 (partial+), CD68 (scattered+), MPO (scattered, focal+)	Peripheral T-cell lymphoma, unspecified type	NA	–
June 4	Bone marrow	Active bone marrow tissue proliferation, significant granulocytic cell proliferation	–	NA	June 3 CHOEP
June 12	Lymph node (pathological consultation)	Ki67(+,80 %),TDT(+),CD4(+),CD8(+),CD3(+), CD5(+),CD45(+)	T-cell lymphoblastic lymphoma	NA	July 16 BFM October 17 BFM-90
November 8	Bone marrow (lymphoma cells comprise 74 %)	Predominantly abnormal immature monocytes with CD56 misexpression, expressing HLA-DR, CD64, CD11c, CD4, CD33, CD38, partial expression of CD9, dim CD123, dim CD15, CD13, CD56, CD11b, minimal expression of CD14	T-Lymphoblastic Lymphoma with rapid marrow infiltration, AML-M5b subtype.	NA	–
November 19	Bone marrow (immature monocytes comprise 67.5 %)	Malignant immature monocytes expressing MPOdim, CD33, CD11b, HLA-DR, CD64, CD11c, CD15, CD38, CD371, CD123, CD4, CD36, partial expression of CD13, CD56, no expression of CD22, cCD3, CD34, CD7, CD117, CD3, CD14, CD96, CD110, CD5, CD2, CD61, CD42a, CD9, cCDT, CD24	AML-M5b	MLL-AF9 fusion gene positive	–
November 26	Bone marrow (immature monocytes comprise 69 %)	–	AML-M5b	46,XY,t(9; 11) (p22; q23)	November 26 IDA

Availability of data and materials

The datasets used and/or analysed during the current study are available from the corresponding author on reasonable request.

Declaration of competing Interest

The authors declare that they have no conflict of interest.

Acknowledgements

The author(s) declare financial support was received for the research, authorship, and/or publication of this article. This work was supported by Sichuan Science and Technology Program (2024NSFSC1292 and 2021YJ0145); the incubation program of General Hospital of Western Theater command (2021-XZYG-C45 and 2021-XZYG-C46) and the general program of General Hospital of Western Theater Command (NO. 2021-XZYGB32).

References

[1] Burkhardt, B. and M.L. Hermiston, Lymphoblastic lymphoma in children and adolescents: review of current challenges and future opportunities. Br. J. Haematol. . 185(6): p. 1158-1170.
[2] A. Kohlmann, et al., New insights into MLL gene rearranged acute leukemias using gene expression profiling: shared pathways, lineage commitment, and partner genes, Leukemia 19 (6) (2005) 953–964.
[3] D.I.A. Grimwade, B.J. Huntly, Molecular landscape of acute myeloid leukemia in younger adults and its clinical relevance, Blood 127 (1) (2016) 29–41. Jan 7.
[4] Y. Wang, et al., The Wnt/beta-catenin pathway is required for the development of leukemia stem cells in AML, Science 327 (5973) (2010) 1650–1653.
[5] Z. Wang, et al., Glycogen synthase kinase 3 in MLL leukaemia maintenance and targeted therapy, Nature 455 (7217) (2008) 1205–1209.
[6] W.J. Harris, et al., The histone demethylase KDM1A sustains the oncogenic potential of MLL-AF9 leukemia stem cells, Cancer Cell 21 (4) (2012) 473–487.
[7] M. Ye, et al., Hematopoietic differentiation is required for initiation of acute myeloid leukemia, Cell Stem Cell 17 (5) (2015) 611–623.
[8] K. Lv, et al., CBL family E3 ubiquitin ligases control JAK2 ubiquitination and stability in hematopoietic stem cells and myeloid malignancies, Genes Dev. 31 (10) (2017) 1007–1023.
[9] H. Makishima, et al., Mutations of e3 ubiquitin ligase cbl family members constitute a novel common pathogenic lesion in myeloid malignancies, J. Clin. Oncol. 27 (36) (2009) 6109–6116.
[10] R. Bejar, et al., Clinical effect of point mutations in myelodysplastic syndromes, N. Engl. J. Med. 364 (26) (2011) 2496–2506.
[11] J. Schwaab, et al., Activating CBL mutations are associated with a distinct MDS/MPN phenotype, Ann. Hematol. 91 (11) (2012) 1713–1720.
[12] M.A. Caligiuri, et al., Novel c-CBL and CBL-b ubiquitin ligase mutations in human acute myeloid leukemia, Blood 110 (3) (2007) 1022–1024.
[13] M.L. Loh, et al., Mutations in CBL occur frequently in juvenile myelomonocytic leukemia, Blood 114 (9) (2009) 1859–1863.
[14] E. Padron, et al., An international data set for CMML validates prognostic scoring systems and demonstrates a need for novel prognostication strategies, Blood Cancer J. 5 (7) (2015) e333, e333.
[15] M. Sanada, et al., Gain-of-function of mutated C-CBL tumour suppressor in myeloid neoplasms, Nature 460 (7257) (2009) 904–908.